Pres. PAC'09 Conf., Vancouver, BC
4-8 May (2009)

BNL 90592-2009-CP

3D SIMULATIONS OF SECONDARY ELECTRON GENERATION AND TRANSPORT IN A DIAMOND ELECTRON BEAM AMPLIFIER*

R. Busby, D.A. Dimitrov, and J.R. Cary
Tech-X Corporation
Boulder, CO 80303

I. Ben-Zvi, X. Chang, J. Keister, E. Muller, **T. Rao, J. Smedley**, and Q. Wu
Brookhaven National Laboratory
Upton, NY 11973-5000

May, 2009

*This manuscript has been authored by Brookhaven Science Associates, LLC under Contract No. DC-AC02-98CH10886 with the U.S. Department of Energy. The United States Government retains, and the publisher, by accepting the article for publication, acknowledges, a world-wide license to publish or reproduce the published form of this manuscript, or allow others to do so, for the United States Government purposes.

DISCLAIMER

This work was prepared as an account of work sponsored by an agency of the United States Government. Neither the United States Government nor any agency thereof, nor any of their employees, nor any of their contractors, subcontractors, or their employees, makes any warranty, express or implied, or assumes any legal liability or responsibility for the accuracy, completeness, or any third party's use or the results of such use of any information, apparatus, product, or process disclosed, or represents that its use would not infringe privately owned rights. Reference herein to any specific commercial product, process, or service by trade name, trademark, manufacturer, or otherwise, does not necessarily constitute or imply its endorsement, recommendation, or favoring by the United States Government or any agency thereof or its contractors or subcontractors. The views and opinions of authors expressed herein do not necessarily state or reflect those of the United States Government or any agency thereof.

3D SIMULATIONS OF SECONDARY ELECTRON GENERATION AND TRANSPORT IN A DIAMOND ELECTRON BEAM AMPLIFIER *

R. Busby, D. A. Dimitrov†, J. R. Cary, Tech-X Corp., Boulder, CO 80303, USA
I. Ben-Zvi, X. Chang, J. Keister, E. Muller, T. Rao, J. Smedley, Q. Wu, BNL, Upton, NY 11973, USA

Abstract

The Relativistic Heavy Ion Collider (RHIC) contributes fundamental advances to nuclear physics by colliding a wide range of ions. A novel electron cooling section, which is a key component of the proposed luminosity upgrade for RHIC, requires the acceleration of high-charge electron bunches with low emittance and energy spread. A promising candidate for the electron source is the recently developed concept of a high quantum efficiency photoinjector with a diamond amplifier [1]. To assist in the development of such an electron source, we have implemented algorithms within the VORPAL particle-in-cell framework for modeling secondary electron and hole generation, and for charge transport in diamond. The algorithms include elastic, phonon, and impurity scattering processes over a wide range of charge carrier energies. Results from simulations using the implemented capabilities will be presented and discussed.

INTRODUCTION

A new concept for a photo-cathode with a diamond amplifier was recently proposed [1] and is currently under active development [2, 3]. The diamond amplified photocathode (DAP) has demonstrated the potential to address the need for high peak and average current, high brightness and low thermal emittance electron beams in current and future accelerator-based systems. Moreover, the DAP has negligible contamination problems, requires two orders of magnitude less laser power, and is expected to have a long lifetime in comparison to existing photo-cathodes.

The idea for the DAP operation consists of generating first a beam of electrons using a conventional photocathode. These are the primary electrons that are accelerated to energies of about 10 keV before impacting a diamond window. When these primary electrons enter into the diamond, they experience inelastic scattering processes leading to the generation of secondary electrons and holes. Any secondary electron or a hole that is produced with a sufficiently high energy can also participate in such inelastic processes, generating more electron-hole (e-h) pairs. These inelastic scattering processes continue until none of the free electrons and holes has sufficiently high energy to generate additional e-h pairs. However, the total number of produced secondary electrons is generally much larger than the number of primary electrons. The free charged carriers also experience inelastic scattering involving the emission or absorption of phonons (lattice excitations). If an external field is applied in the diamond, the free electrons and holes will start drifting in opposite directions. Large numbers of the secondary electrons are transported through the diamond and emitted from one of its surfaces. Diamond emission surfaces are prepared to have a negative electron affinity (NEA) in order to increase the emission. The electrons are emitted into the accelerating cavity of an electron gun.

To optimize the performance of the DAP concept, it is of considerable interest to understand the generation of secondaries and their transport in diamond samples with different characteristics (thickness, concentration and type of impurities, surface effects at both metal coated and NEA surfaces) and how a diamond amplifier couples to the overall operation of the complete photoinjector system. To address this problem, we have been developing models, within the VORPAL [4] computational framework, for simulation of secondary electron generation and charge transport in diamond. Initially, we implemented models for the inelastic scattering leading to generation of secondary electrons and holes [5]. Here, we report on our work to enable the simulation of charge transport in diamond. The ability to simulate both secondary electron generation and charge transport allows us to investigate electron gain from diamond in a transmission mode setup (D. A. Dimitrov *et al.* in these proceedings).

MODELING SECONDARY ELECTRON GENERATION AND TRANSPORT

The short time scale (of the order of 100 fs) dynamics of electrons in diamond with medium range of energies (from about 50 eV to 10 keV) was treated by considering elastic and inelastic scattering processes, with the latter leading to generation of secondary electrons and holes [6, 7, 8]. For the inelastic scattering, we implemented first the Ashley model described by Ziaja *et al.* [6, 7] and considered secondary electron generation effects with it [5]. Recently, we also implemented the TPP-2 optical model for the inelastic scattering that produces scattering rates in better agreement [8] with the rates from band-structure calculations [9] at low energies ($\sim$ 10 eV). For the elastic scattering in the medium energy range we used the rates given in Ref. [8] but our implementation [5] is based on methods from semiconductor device simulations [10]. The scattering rates for the elastic and the inelastic (calculated with

* We are grateful to the US DoE for supporting this work under the DE-FG02-06ER84509 grant.
† dad@txcorp.com

the TPP-2 model) processes are shown in the top plot of Fig. 1.

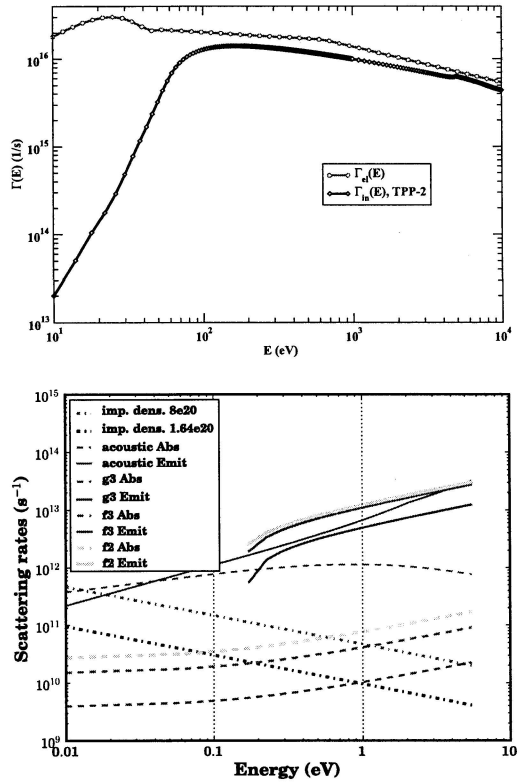

Figure 1: The top plot shows the inelastic scattering rates for generation of secondary electrons and holes (calculated from the TPP-2 model) together with the elastic rates in the medium energy range. The bottom plot shows the rates for electron-phonon (low energy inelastic) and impurity (elastic) scattering processes.

The free (conduction band) electrons in diamond also experience low-energy inelastic scattering with phonons (lattice excitations) and elastic scattering from charged impurities. Charge transport cannot be simulated accurately without including the electron-phonon scattering. These inelastic processes lead to additinal relaxation of the the electron energies to reach the drift state in an applied field. At low fields, free electrons have energies close to the bottom of the conduction band and drift with temperature effectively equal to the temperature of the diamond crystal (a highly desirable property for generation of beams with low thermal emittance).

For the low-energy inelastic scattering with optical and acoustic phonons we implemented Monte Carlo algorithms based on the models given by Jacoboni and Reggiani [11]. In diamond, these models approximate the energy bands with a parabolic dependence on the electron wave vector and have ellipsoidal constant energy surfaces. Both intervalley and intravalley electron-phonon processes are included. The rates for the emission and absorption of acoustic phonons and the three optical phonons considered are shown in the bottom plot of Fig. 1 at $T = 300$ K. The g and f type rates are for transitions between parallel and perpendicular valleys, respectively. Decreasing the temperature of diamond reduces these rates [11]. For comparison, the rates for scattering of electrons from charged impurities (using the model from Ref. [11]) at two concentrations is also shown together with the electron-phonon scattering rates. The data plotted in Fig. 1 shows that in the medium electron energy range, the rates for secondary electron generation and for elastic scattering are several orders of magnitude larger than the electron-phonon and charged impurity scattering ones. However, at low electron energies (10 eV and lower) the secondary electron generation rates are comparable to the electron-phonon rates. Note that modeling of electron transport with energies close to the bottom of the conduction band does not include elastic scattering [9] from the periodic potential of the carbon ions as done for the medium energy range [6].

We have implemented a general Monte Carlo algorithm to handle all scattering processes (it also includes null collisions [10] to increase the efficiency). In between scattering events, the particle-in-cell algorithms in VORPAL [4] provide the capability to self-consistently move particles interacting with electromagnetic fields.

ELECTRON TRANSPORT SIMULATIONS

In this Section, we discuss representative results from simulations with the implemented models on electron transport after secondary electrons and holes are generated using one of the models for inelastic scattering. We used the Ashley model for the results here and primary electron energy of 2.7 keV. We reported effects related to the secondary electron generation with this model in a previous study [5] and present only new results from the transport simulations here.

The domain was split into a three-dimensional grid, typically of $24 \times 24 \times 24$ cells, with a cell edge size of 0.1 μm. For the simulations described here, a small time step (usually 8×10^{-18} s) was used during the creation of the secondary electrons (to resolve the mean free time for these processes) which happens during the first few hundred femtoseconds. Phonon scattering was not enabled during this time interval. At the end of this interval, the VORPAL data was dumped, the input file modified to increase the time step (for faster simulation runs while still resolving the mean free times of the low energy scattering processes), and to enable scattering of the free charged carriers with phonons. The total propagation time of these simulations was approximately 20 ps.

We specifically studied the dependence of the drift velocity obtained with the phonon scattering models on the applied external field magnitudes in a range values from 0.05 to 10 MV/m. This is a range of interest for use in diamond amplified photo-cathodes. Our goal was to verify that the models can describe the transport of electron

clouds with drift velocities in agreement with experimental measurements for this range of applied fields.

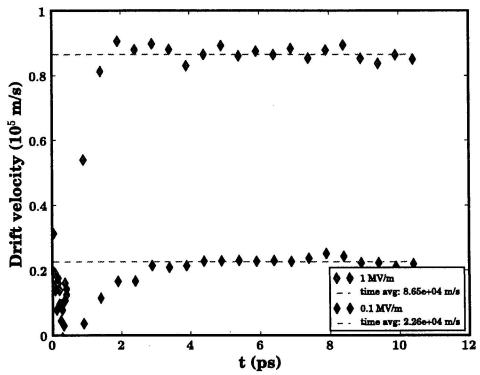

Figure 2: The drift velocity evolution at two applied fields indicate the rate of convergence to the (time) average values (given in the legend).

The relaxation behavior of the drift velocity to steady state from simulations at two field values is shown Fig. 2. The results show that it takes of the order of a few picoseconds to reach the steady state. The relaxation time decreases when increasing the applied field.

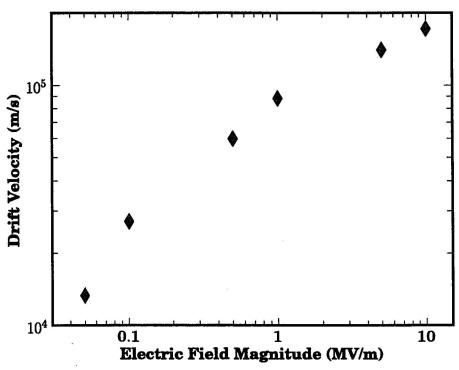

Figure 3: The obtained average electron drift velocity vs applied field from VORPAL simulations of electron transport in diamond agrees well with experimental data.

The dependence of the average electron drift velocity on the applied field magnitude obtained from the VORPAL simulations with the models we implemented for the electron-phonon scattering is shown in Fig. 3. These values agree well with experimental data and the more detailed, band-structure Monte Carlo simulation results given by Watanabe *et al.* [9].

SUMMARY

We described here the overall modeling capabilities we have implemented within the VORPAL computational framework for simulation of secondary electron generation and transport in diamond. We presented results from transport simulations to determine the electron drift velocity dependence on the applied field. These simulations test the implemented electron-phonon scattering models. The drift velocity obtained from VORPAL agrees well with experimental data and more detailed band-structure calculations for the fields of interest. This gives us confidence that the electron-phonon models we implemented in VORPAL are adequate to simulate electron transport in diamond for studying DAP properites. In future developments, we will investigate how to incorporate models of electron emission from diamond surfaces with negative electron affinities and effects related to trapping of electrons in diamond.

REFERENCES

[1] I. Ben-Zvi, X. Chang, P. D. Johnson, J. Kewisch, and T. Rao. Secondary emission enhanced photoinjector. C-AD Accelerator Physics Report C-A/AP/149, BNL, 2004.

[2] X. Chang, I. Ben-Zvi, A. Burrill, S. Hulbert, P. D. Johnson, J. Kewisch, T. Rao, J. Smedley, Z. Segalov, and Y. Zhao. Measurement of the secondary emission yield of a thin diamond window in transmission mode. In C. Horak, editor, *2005 Particle Accelerator Conference. IEEE*, number 2251-3, 2005.

[3] X. Chang, I. Ben-Zvi, A. Burrill, J. Grimes, T. Rao, Z. Segalov, J. Smedley, Q. Wu Recent Progress on the Diamond Amplified Photo-cathode Experiment In *2007 Particle Accelerator Conference. IEEE*, pp. 2044-6, 2007.

[4] C. Nieter and J. R. Cary. VORPAL: a versatile plasma simulation code. *J. Comput. Phys.*, 196:448–473, 2004.

[5] D. A. Dimitrov, R. Busby, D. L. Bruhwiler, J. R. Cary, I. Ben-Zvi, T. Rao, X. Chang, J. Smedley, Q. Wu 3D Simulations of Secondary Electron Generation and Transport in a Diamond Amplifier for Photocathodes In *2007 Particle Accelerator Conference. IEEE*, pp. 3555-7, 2007.

[6] B. Ziaja, D. van der Spoel, A. Szöke, and J. Hajdu. Auger-electron cascades in diamond and amorphous carbon. *Phys. Rev. B*, 64(214104-1/8), 2001.

[7] B. Ziaja, A. Szöke, D. van der Spoel, and J. Hajdu. Space-time evolution of electron cascades in diamond. *Phys. Rev. B*, 66:024116–1/9, 2002.

[8] B. Ziaja, R. A. London, and J. Hajdu. Unified model of secondary electron cascades in diamond. *J. Appl. Phys.*, 97:064905–1/9, 2005.

[9] T. Watanabe, T. Teraji, T. Ito, Y. Kamakura, and K. Taniguchi Monte Carlo simulations of electron transport properties of diamond in high electric fields using full band structure *J. Appl. Phys.* 95:4866-74, 2004.

[10] M. Lundstrom. *Fundamentals of Carrier Transport.* Cambridge University Press, second edition, 2000.

[11] C. Jacoboni and L. Reggiani The Monte Carlo method for the solution of charge transport in semiconductors with applications to covalent materials *Rev. Mod. Phys.*, 64:645-705, 1983.